Figure 2: Amino acid sequence of human ChemR23 (371 amino acids) (SEQ ID NO 2). The seven predicted transmembrane domaines are underlined. The consensus sequence for *N*-linked glycosylation (N-X-S/T) in the N terminus is bold and the potential site of phosphorylation by PKC (S/T-X-R/K) in the C terminus is in italic.

MEDEDY**NTS**ISYGDEYPDYLDSIVVLEDLSPLEARVTRIFLVVVYSIVCFLGILGNGLVIIIAT
FKMKKTVNMVWFLNLAVADFLFNVFLPIHITYAAMDYHWVFGTAMCKISNFLLIHNMFTSVFLL
TIISSDRCISVLLPVWSQNHRSVRLAYMACMVIWVLAFFLSSPSLVFRDTANLHGKISCFNNFS
LSTPGSSSWPTHSQMDPVGYSRHMVVTVTRFLCGFLVPVLIITACYLTIVCKLQRNRLAKTKKP
FKIIVTIIITFFLCWCPYHTLNLLELHHTAMPGSVFSLGLPLATALAIANSCMNPILYVFMGQD
FKKFKVALFSRLVNALSEDTGHSSYP*SHR*SFTKMSSMNERTSMNERETGML

Figure 2: Amino acid sequence of human ChemR23 (371 amino acids) (SEQ ID NO 2).

MEDEDY**NTS**ISYGDEYPDYLDSIVVLEDLSPLEARVTRIFLVVVYSIVCFLGILGNGLVIIIAT
FKMKKTVNMVWFLNLAVADFLFNVFLPIHITYAAMDYHWVFGTAMCKISNFLLIHNMFTSVFLL
TIISSDRCISVLLPVWSQNHRSVRLAYMACMVIWVLAFFLSSPSLVFRDTANLHGKISCFNNFS
LSTPGSSSWPTHSQMDPVGYSRHMVVTVTRFLCGFLVPVLIITACYLTIVCKLQRNRLAKTKKP
FKIIVTIIITFFLCWCPYHTLNLLELHHTAMPGSVFSLGLPLATALAIANSCMNPILYVFMGQD
FKKFKVALFSRLVNALSEDTGHSSYP*SHR*SFTKMSSMNERTSMNERETGML

Figure 5: Alignment of ChemR23

Alignment of the amino acid sequence of ChemR23 with AT2 receptors, C3a, C5a and fMLP receptor and other chemoattractants related sequences were performed using ClustalX algorithm. Then, the dendrogram was constucted using TreeView algorithm.

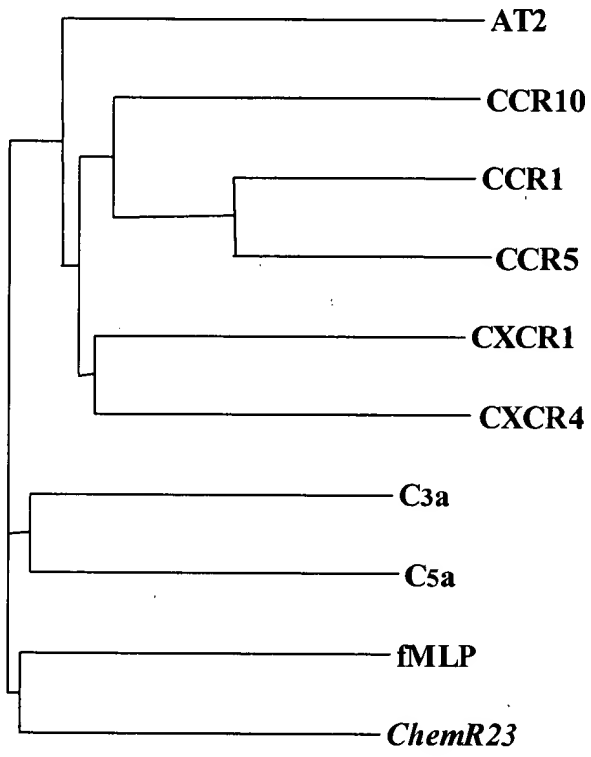

Figure 5: Alignment of ChemR23

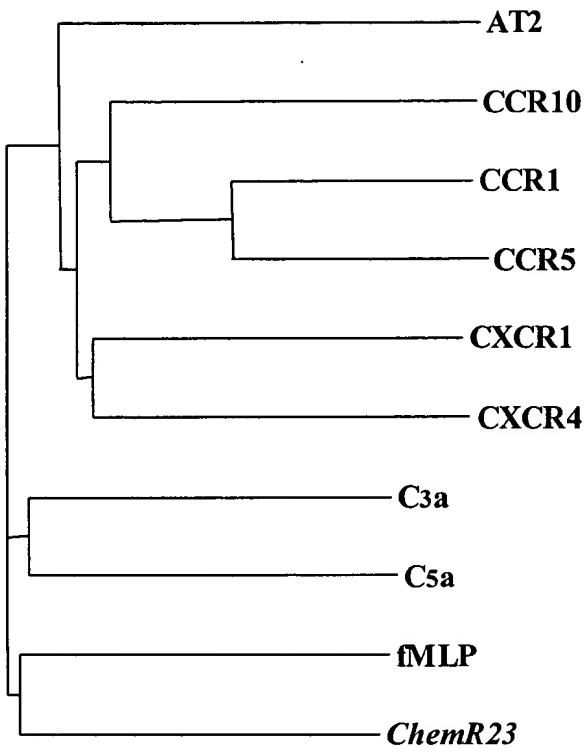

Figure 8: Amino acid sequence alignment of human and mouse TIG2. Identical and similar residues are shaded.

Figure 8: Amino acid sequence alignment of human and mouse TIG2.

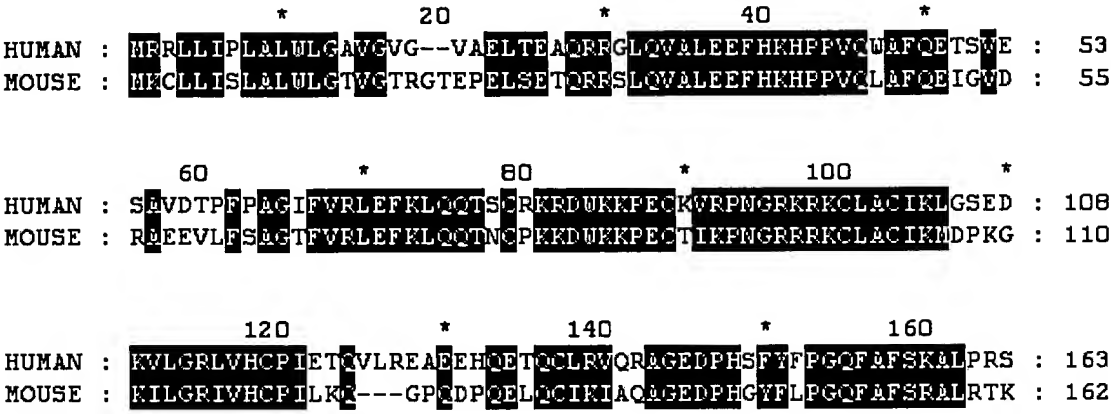

Figure 10: Primary screening of HPLC fractions obtained from the fractionation of human ovary ascites.

The different fractions obtained following fractionation of human ovary ascites were diluted fivefold in the buffer assay and tested in aequorin assay using a cell line expressing ChemR23 (open circles) or cell lines expressing not related receptors (closed triangles and squares). The response obtained for each fraction was normalized using the ATP response of each cell line.

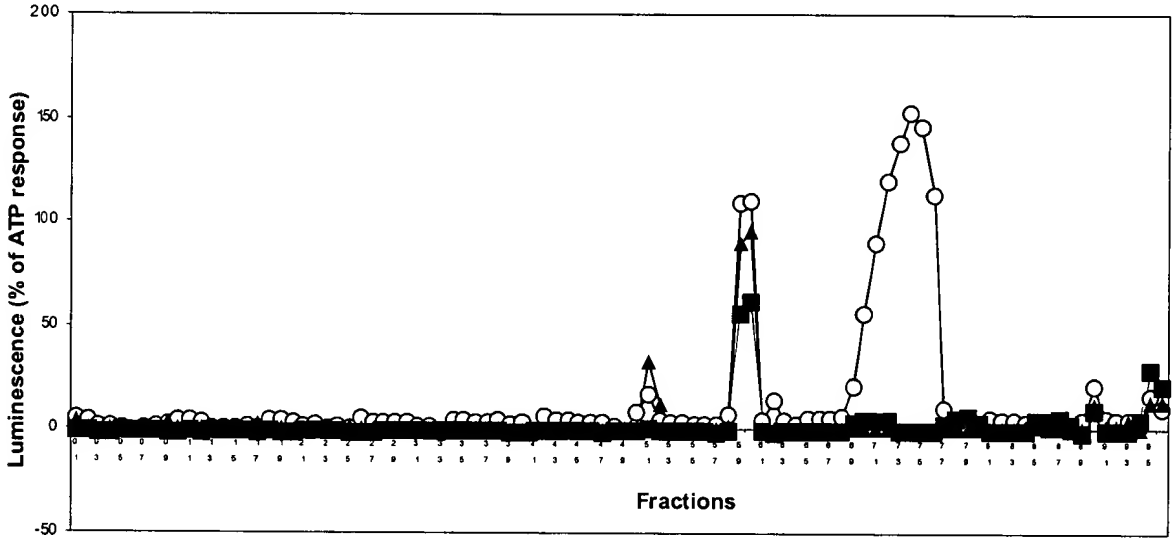

Figure 10: Primary screening of HPLC fractions obtained from the fractionation of human ovary ascites.

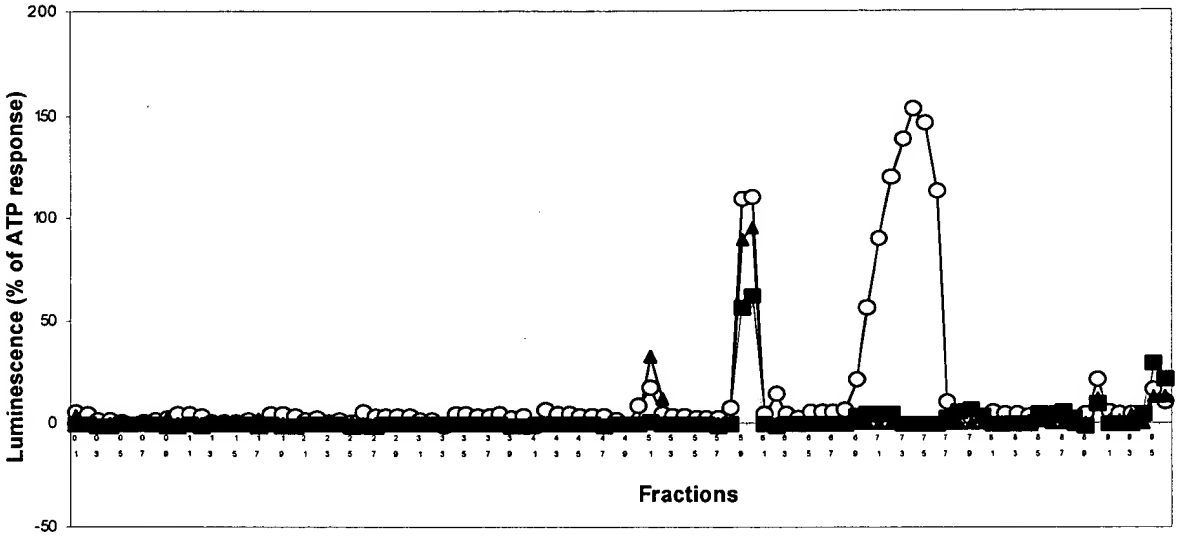

Figure 11: Activation of ChemR23 by cells transfected with TIG2

293 T cells were transiently transfected with pCDNA3- TIG2 or with pCDNA3 alone (mock transfected). Increasing volumes of the supernatant collected 4 days following transfection were analysed in a aequorin-based assay with CHO cells expressing ChemR23. A representative experiment is shown. Assay was performed in triplicate and SD are indicated.

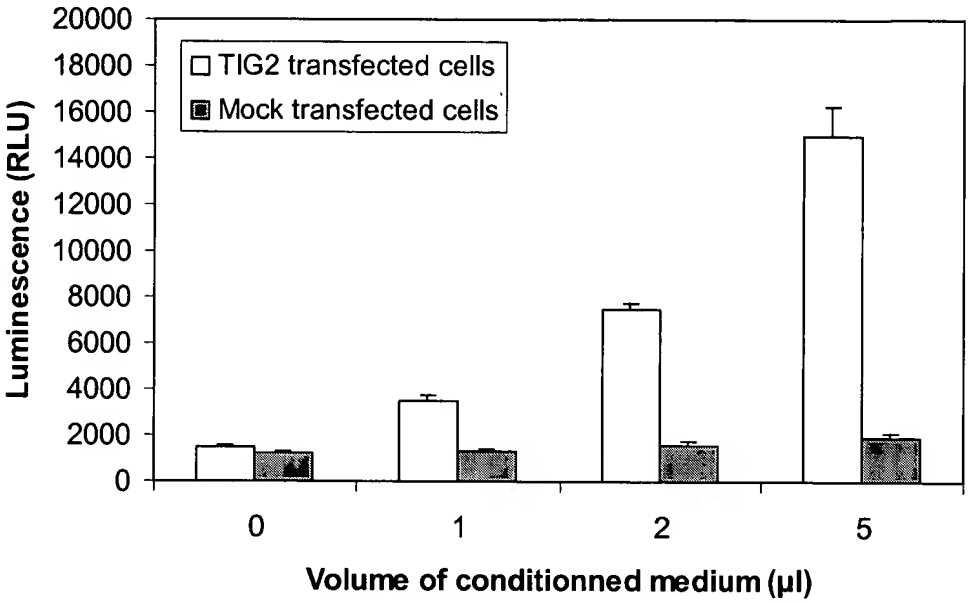

Figure 11: Activation of ChemR23 by cells transfected with TIG2

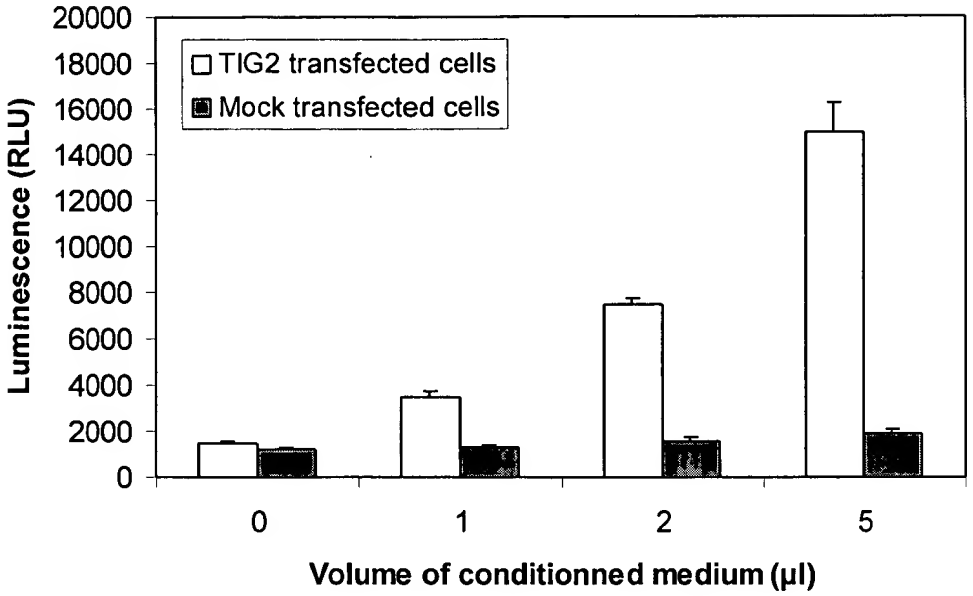

Figure 12; Characterization of antibodies directed against ChemR23

A mixture of recombinant cells made up of 2/3 recombinant ChemR23 CHO cells and 1/3 recombinant HCR CHO cells (negative control) was subject to react with either a supernatant of the anti ChemR23 5C 1H2 monoclonal antibody (thick line) or a supernatant with no known antibody activity (thin line, grey filling). After staining with FITC labeled anti mouse Ig these preparations were analysed by flow cytofluorometry. Results are displayed as a histogram of the number of cells (Events axis) expressing a given fluorescence (FL1-H axis). Monoclonal 5C 1H2 allowed to discriminate the ChemR23 recombinant sub-population of cells from the negative control cells as evidenced by the relative proportions of both type of cells. The background fluorescence of the assay is given by the second staining (grey filling).

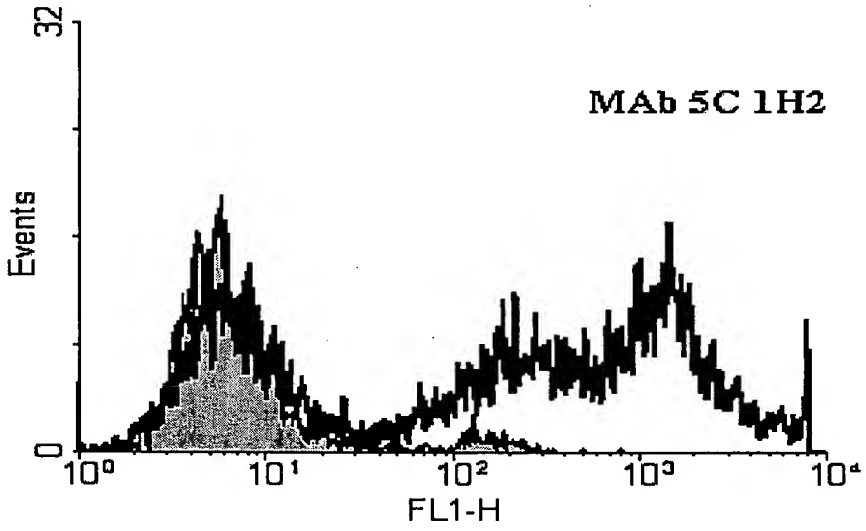

Figure 12: Characterization of antibodies directed against ChemR23